ENVIRONMENTAL EFFECTS ON VIABLE VIRUS TRANSPORT AND RESUSPENSION IN VENTILATION AIRFLOW

A Thesis

by

TATIANA ANABELLE BAIG

Submitted to the Graduate and Professional School of
Texas A&M University
in partial fulfillment of the requirements for the degree of

MASTER OF SCIENCE

Chair of Committee,	Maria King
Committee Members,	Sandun Fernando
	Mark Kimber
Head of Department,	John Tracy

December 2021

Major Subject: Biological and Agricultural Engineering

ABSTRACT

Currently little is known on how SARS-CoV-2 spreads indoors and its infectability. The objective of this study is to gain more knowledge on the effect of environmental factors on the spread and infectivity of virus aerosols in the built environment. Understanding how the virus transmits indoors would allow for early detection and mitigation of viral particles in room sized spaces. Bovine coronavirus (BCoV) was used as virus simulant in laboratory experiments conducted in a controlled humidity cabinet at Biosafety Level 2. An air-jet nebulizer was used to disseminate known numbers of BCoV particles. After aerosolization, the surface in the cabinet was swiped at regular time intervals to assess the number of particles impacted. Additional surfaces placed in the chamber and swiped at the end of testing. The samples were quantified using quantitative polymerase chain reaction (qPCR). Virus attachment to the surfaces was analyzed using bio-layer interferometry. The virus aerosols that remained suspended in the air were collected bioaerosol collectors with a reference air sampler and quantitated by qPCR. To monitor the effect of the ventilation on the virus movement, PRD1 bacteriophage aerosols as virus simulants were also disseminated in a ¾ scale ventilated hospital test room equipped with twelve PM2.5 samplers at 15 L/min. After plating and counting the plaque forming units (PFU), the highest concentration of viral particles was detected above the patient's head in the test room in the second ventilation configuration. Other high virus concentration locations were near the foot of the patient's bed. From these results, it was determined that with the current airflow set up in the second configuration with the air inlet on the ceiling above the bed, exhaust bottom left on the wall behind the bed, the virus particles concentrate over the lower part of the patient's bed. Based on air property measurements, aerosol collections and the mechanical blueprint of the model room, a computational flow model was created to visualize the entrainment and movement of the virus in the ventilation airflow. The models showed the third presented configuration minimized particle concentration at the door while the first configuration decreased overall particle concentration in the room.

ACKNOWLEDGEMENTS

I would like to thank my committee chair, Dr. King, and my committee members, Dr. Fernando and Dr. Kimber, for their guidance and support throughout the course of this research.

Thanks also go to my friends and colleagues and the department faculty and staff for making my time at Texas A&M University a great experience.

Finally, thanks to my mother and father for their continual love and support, my sisters for their encouragements, and my partner for his patience and love.

CONTRIBUTORS AND FUNDING SOURCES

Contributors

This work was supervised by a thesis committee consisting of Dr. Maria King (advisor) and Dr. Sandun Fernando of the Department of Biological and Agricultural Engineering and Dr. Mark Kimber of the Department of Nuclear Engineering.

The data analyzed in Chapter 3.1 was conducted in part by Meiyi Zhang of the Department of Biological and Agricultural Engineering.

All other work conducted for this thesis was completed by the student independently.

Funding Sources

Graduate study was supported by a graduate assistantship from the Department of Biological and Agricultural Engineering at Texas A&M University.

This study was supported by the NSF CBET 2034048 grant. Its contents are solely the responsibility of the authors and do not necessarily represent the official views of the National Science Foundation.

NOMENCLATURE

3D	Three Dimensional
APS	Aminopropylsilane
ANSYS	Analysis System
BCoV	Bovine Coronavirus
BLI	Biolayer Interferometry
CFD	Computational Fluid Dynamics
g	grams or gravitational force
GCN	Gene Copy Number
LB	Luria Bertani
HEPA	High Efficiency Particulate Air
mL	Milliliter
MQ	Milli-Q
PBS	Phosphate-Buffered Saline
PFU	Plaque Forming Units
qPCR	quantitative Polymerase Chain Reaction
SolidWorks	Computer-Aided Design Analysis System
WWC	Wetted Wall Cyclone

TABLE OF CONTENTS

Page

LIST OF FIGURES

LIST OF TABLES

Page

1. INTRODUCTION

A novel human coronavirus, Severe Acute Respiratory Syndrome Coronavirus 2 (SARS-CoV-2) that emerged in Wuhan, China, in December 2019, has now reached a pandemic level of global incidence [1]. The virus can enter the human body through the eyes, mouth, or nose and replicate itself after binding to receptors in the lung and other organs. Studies indicate the SARS-CoV-2 virus can remain viable and infectious suspended in aerosols for hours and on surfaces up to days, enabling efficient aerosol and fomite transmission of SARS-CoV-2 [2-6]. The consensus is that in the real world, droplet transmission that occurs within three to six feet accounts for the vast majority of SARS-CoV-2 transmissions. A recent study showed that 6 feet may not be sufficient to protect against coronaviruses, which may travel up in droplets up to 27 feet, but it was received with skepticism [7]. A single sneeze may emit 40,000 droplets with a geometric mean size of 360.1 μm exhaled immediately at the mouth [8]. Over 87 % of particles exhaled by flu influenza patients were under 1 μm [9]. However, a similar percentage was reported for significantly larger (0.3-0.5 mm) particles exhaled by subjects infected with rhinovirus [10]. A computational model created by Vuorinen et al. [11] within a multi-institutional project shows that a cough from a person in one aisle in a grocery store spreads as a cloud of nanosized particles over the shelves into the next aisle. Similar open-source simulations can be found on the internet for cough aerosols spreading over aisles in an airplane. Earlier studies indicate that human movement in an airplane cabin increases the risk of infections by reducing the overall deposition and removal rate of the suspended aerosols [12].

Hospitals and clinics follow rigorous guidelines to maintain hygiene at 35% - 60% relative humidity (RH) and 21°C - 24°C temperature values (NFPA 99), with a mandated six air exchanges per hour (6 ACH). The role of ventilation in removing exhaled bioaerosols in buildings to prevent cross infections has been extensively studied after the severe acute respiratory syndrome coronavirus (SARS-CoV) outbreak in 2003 and can help inform to mitigation strategies for the current SARS-CoV-2 pandemic [13]. Swabs taken from the air exhaust outlets in a hospital tested positive for SARS-CoV-2, suggesting that small virus-laden droplets may be transported by airflows and deposited on vents [4]. However, due to the limitations of the sampler used in the study, the virus wasn't detected in the airflow. Viable coronavirus (SARS-CoV-2) found on the Diamond Princess Cruise ship surfaces weeks after people were evacuated indicates that the virus survives for longer times on surfaces and forms biofilm-like structures, which may be influenced by environmental conditions [14]. Recent studies reveal that poor air quality and atmospheric pollution may be linked to the spread of the virus resulting in a greater number of COVID-19 cases in polluted areas [15].

Currently little is known on how SARS-CoV-2 spreads indoors and its infectability. The objective of this study was to gain more knowledge on the effect of environmental factors on the spread and infectivity of virus aerosols in the built environment. The goal was to answer fundamental questions about the infectivity and spread of viable viruses in indoor environments using the bioaerosol collectors developed in the aerosol technology laboratory where this study was conducted.

As ventilation systems are practically ubiquitous in common workplaces, the effect of air properties on the infectivity and transport of aerosolized viruses is one of the most important subjects for study to aide in reducing the spread of infectious viral particles. This study is one of the first comprehensive studies of the impact of environmental conditions including temperature, humidity, and air velocity on the droplet size, spread, and deposition of airborne viruses. The identification of optimized environmental conditions and development of optimized ventilation designs could significantly reduce the entrainment and spread of viable infectious viruses in the air. The laboratory's previous work indicates that a combined modeling and sampling approach can be used to mitigate transport of airborne infectious microorganisms in a ventilated facility. Based on the airflow model and the bioaerosol movement, an optimal air intake/exhaust design can be selected that would result in the highest sanitation requirement (i.e. the least number of infectious agents) in the airflow. This thesis study addresses the need for an optimal air intake/exhaust design combined with optimal environmental conditions needed to reduce the amount of SARS-CoV-2 viral particles in the air by integrating aerobiology with particle tracking and computational fluid modeling. Ultimately, this work allows for a better understand of the behavior of virus size particles and a redesign for ventilation systems for reduced virus transmission at facilities, with a potential for application to any built environment.

The outcome of this study has the potential to protect public health through continuous monitoring of viral concentrations, with sufficient throughput to detect dynamic changes in concentration levels in room-size spaces. The potential for efficient

detection of viable virus aerosols and mitigation of their spread was assessed by conducting controlled experimental studies to establish the pattern for aerosolization, deposition, and resuspension of SARS-CoV-2 simulant viruses at different environmental conditions and modeling the airflow pattern in a plexiglass model chamber and a model hospital room to determine the effect of ventilation on the entrainment and spread of virus aerosols.

2. METHODS AND MATERIALS

2.1. Media and Sampler Preparation

The protocol followed for media and sample preparation was from Bonilla et al. [16]. Parts of the protocol were altered to fit the experiment. The soft agar medium was used to plate the phage samples. The collected phage sample and the *Salmonella* host were both pipetted into the soft agar overlay and poured onto a prepared plate. This process was repeated for all the collected samples as well as stock solution dilutions, nebulizer solution dilution, and the exhaust filter sample. The plates were placed in the incubator over night to grow and the plaques formed were counted the next day.

To prepare the Luria Bertani (LB) culture mdium, 10 g of peptone, 5 g of yeast extract, and 5 g of NaCl were added per liter of MQ water and autoclaved. The soft agar medium was prepared by adding 25 g of LB broth and 7.5 g of agar per liter of MQ water. The soft agar was prepared in 50 mL batches and autoclaved.

Salmonella enterica Serovar Typhimurium LT2 (RP1) bacterium was used as the phage host as this strain of *Salmonella* acts as a strong host and allows the PRD1 phage to grow well. The culture medium consisted of LB and 100 mg/L Ampicillin, added after autoclaving. The Ampicillin was used to select for cells that harbor the PRD1 plasmids of Salmonella to maximize phage growth. The SM buffer used during phage isolation and propagation was prepared by adding 5.8 g of NaCl, 2.0 g of $MgSO_4 \cdot 7\ H_2O$, and 50 mL of 1 M Tris-HCl with a pH of 7.4 per 1 liter of MQ water, autoclaved, 0.2 μm filter-sterilized and stored at room temperature. Calcium chloride ($CaCl_2$) solution was prepared as a

filter-sterilized 1 M stock solution to be added to the desired LB broth volume to obtain a final concentration of 0.001 M. The overlay was prepared by adding 0.1 mL of fresh mid-log phase *Salmonella* host culture incubated at 37ºC, and 0.1 mL of phage (10^6 - 10^7 PFU/mL) to 3 mL of soft agar with 100 mg/L Ampicillin at 56ºC in a 5 mL tube, pouring it over a Tryptic Soy Agar (TSA) plate and incubating it overnight at 37ºC.

2.1.1. Phage isolation and propagation via plate lysate

A single phage plaque was picked from a plate lysate plate with a sterile pipet, resuspended in a microcentrifuge tube with 1 mL of filter-sterilized SM buffer, and vortexed for 5 min. This solution was then centrifuged at 4,000 x g for 5 min to remove agar particles. After incubating the plate at 37°C, the plate was lysed by pouring 5 mL of SM buffer on top of the plate and shaking, gently, for 15 min. The buffer was collected and centrifuged at 4,000 x g for 5 min. The phage lysate was stored at 4 °C.

2.2. Plexiglass Model Chamber Test

In a controlled plexiglass model chamber at Biosafety Level 2, an air-jet nebulizer was used to disseminate known numbers of bovine coronavirus (BCoV) aerosols. BCoV, an enveloped, positive-sense, single-stranded RNA virus is a betacoronavirus similar to SARS-CoV-2 that served as the simulant virus throughout this study which allowed for generalization of results to SARS-CoV-2. A series of experiments were performed at different temperatures and humidity values to assess the effect of environmental factors on the particle deposition. At regular time intervals after aerosolization, the cabinet

surfaces were sampled to quantify the number of impacted viral particles using cell culture and quantitative polymerase chain reaction (qPCR). The viable and total virus concentrations that were resuspended in the air were assessed using the bioaerosol collectors with a refence sampler and with qPCR.

2.2.1. Plexiglass model chamber set-up

A controlled temperature - humidity BSL-2 chamber (57.9 cm x 45.4 cm x 40.3 cm) (Fig. 1**)** was built of clear Plexi-glass Polypropylene. A Collison 6-jet nebulizer (BGI, Waltham, MA) was used to disseminate known numbers of BCoV aerosols at different relative humidity (30, 60 and 80%) and temperature (10, 15, 25ºC) values monitored by probes. The range of temperature and relative humidity values was based on the measurements the authors conducted in meat processing facilities in preliminary studies. A fan with a HEPA filter (to provide particle free background air) and a flow straightener was connected to the inlet to maintain the airflow at approximately 0.1 m/s in the chamber, corresponding to the average indoor air velocity [17]. An additional HEPA filter was inserted at the chamber exit. HOBO dataloggers and hot wire anemometer (TSI Inc., Burnsville, MN) were used for temperature, relative humidity, and air velocity measurements.

The number of impacted viral particles on the walls and metal, plastic, and wood surface samples (2 in. x 1 in.) at the bottom of the chamber were quantitated to assess the effect of humidity and temperature on particle deposition. The virus concentration that remained resuspended was quantitated using the impinger-type Wetted Wall Cyclone

(WWC) bioaerosol collectors, with stainless steel and 3D-printed cyclones, respectively, operated at 100 L/min. As an impaction-type collector, the MD8 Sartorius Airport Sampler was operated at 50 L/min, using 80 mm gelatin filters as reference. Each test was repeated three times.

2.2.2. Virus quantitation by qPCR

For total viral counts for all samples, whole cell qPCR (quantitative Polymerase Chain Reaction) was performed using BCoV specific oligonucleotides and probes [18]. Virus RNA was extracted from aliquots of the collected bioaerosol samples to synthesize cDNA using the Goldbio Reverse Transcriptase Kit [19]. The BCoV cDNA was added to the qPCR SYBR Green reaction mixture (Applied Biosystems, Warrington, UK), and amplified in an automated thermocycler/analyzer (AB StepOne RT-PCR System, AB, Foster City, CA) as described previously [20]. Broadly reactive primer pairs IN-2 (+) 5' GGGTTGGGACTATCCTAAGTGTGA 3' and IN-4 (–) 5' TAACACACAACICCATCATCA 3' were used to identify bovine coronavirus (GenBank Access NC_003045). Dilutions of a plasmid containing the BCoV target sequence was used to create a standard calibration curve for each analysis and allow for calculation of total viral gene copy number [21].

2.2.3. Surface virus assessment

Three different surfaces were placed inside the chamber: plastic, wood and metal. Polypropylene, chemical compound shown in Fig. 1 [25], was the plastic surface used in

the chamber. The wood surface has a varnish finish made of polyurethane, Fig. 2 [26]. The metal surface used was aluminum. Fig. 3 shows the chemical compound of the plexiglass chamber, polymethyl methacrylate [27].

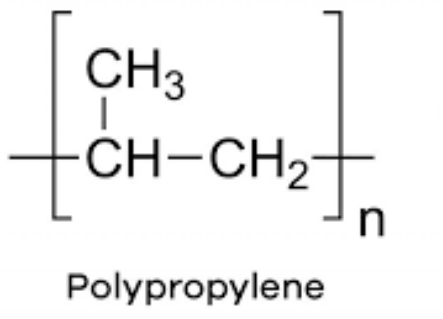

Figure 1 Chemical compound of polypropylene

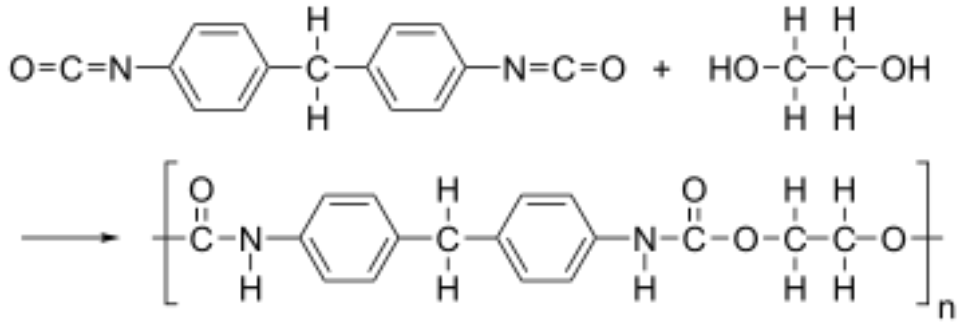

Figure 2 Chemical compound of polyurethane

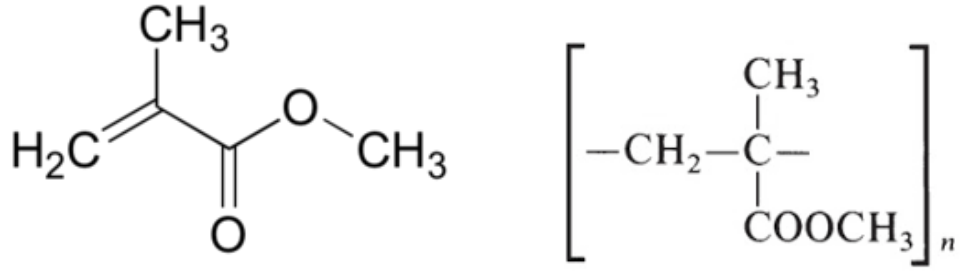

Figure 3 Chemical compound of methyl methacrylate (left) and a poly group (right)

Bio-layer interferometry (BLI) was performed on the surface swab samples to determine the kinetics of the samples collected for each surface under the different environmental conditions. BLI is a technique used to measure the micromolar interactions through white light interference cause by the sample attaching to the biosensor surface. The BLItz system (ForteBio) was used for the testing with APS biosensors. Each biosensor was hydrated in PBS buffer for 10 minutes before use. The tests had 3 steps, baseline, association, and dissociation. The baseline step was performed with 4 µL of PBS buffer for 30 sec. The association step used 4 µL of sample for 300 sec to allow the sample to associate to the surface and measure the association of the sample to the biosensor surface. Dissociation took 300 sec with 4 µL of PBS buffer to allow the sample to dissociate from the surface and measure the sample dissociation from the biosensor surface. The BLItz system was used to generate binding curves with local modeling using a designated reference. Based on the curve the association and dissociation rates and kinetics constants were determined for each surface swab sample.

2.3. ¾ Scale Hospital Room Test

2.3.1. Hospital room and equipment set-up

The Texas A&M University Biosafety Level 2, air conditioned, ¾ scale physical particle test room operated at an air exchange rate of 6 air changes per hour (ACH) was utilized to test PRD1 phages as SARS-CoV-2 simulants. Twelve PM2.5 filter samplers at 15 L/min air flow were used to collect the aerosolized virus (Fig. 4 and Fig. 5) [22]. Tests were conducted using three different ventilation configurations (Fig. 5).

During sampling, environmental conditions (temperature, humidity, air velocity) were monitored. The virus particles were injected into the chamber with a Collison 24 jet atomizer at a location by the wall where the head of a breathing person in the room would be typically located. A 50 mL aliquot of the phage sample was added to 300 mL of SM buffer and nebulized as a SARS-CoV-2 simulant. Twelve PM2.5 samplers with HTTP 0.4 µm membrane filters (VWR) were placed in the model room to sample air at 15 L/min inflow rate. The filter at the air exhaust was also collected and anlyzed after each test. Sampling was conducted at room temperature during the entire period of 5 min nebulization. Each test was repeated 3 times.

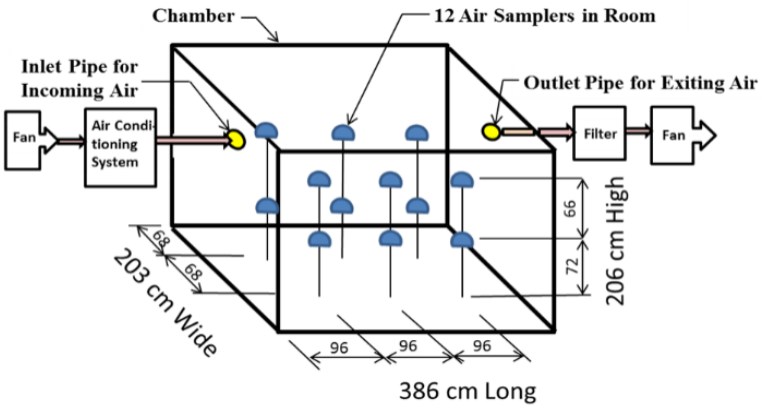

Figure 4 Hospital model room dimensions and locations of the PM2.5 Samplers. A, C, E, G, I, and K are all upper samplers (138 cm above ground and 66 cm above lower samplers). The lower samplers are B, D, F, H, J, and L (72 cm above ground).

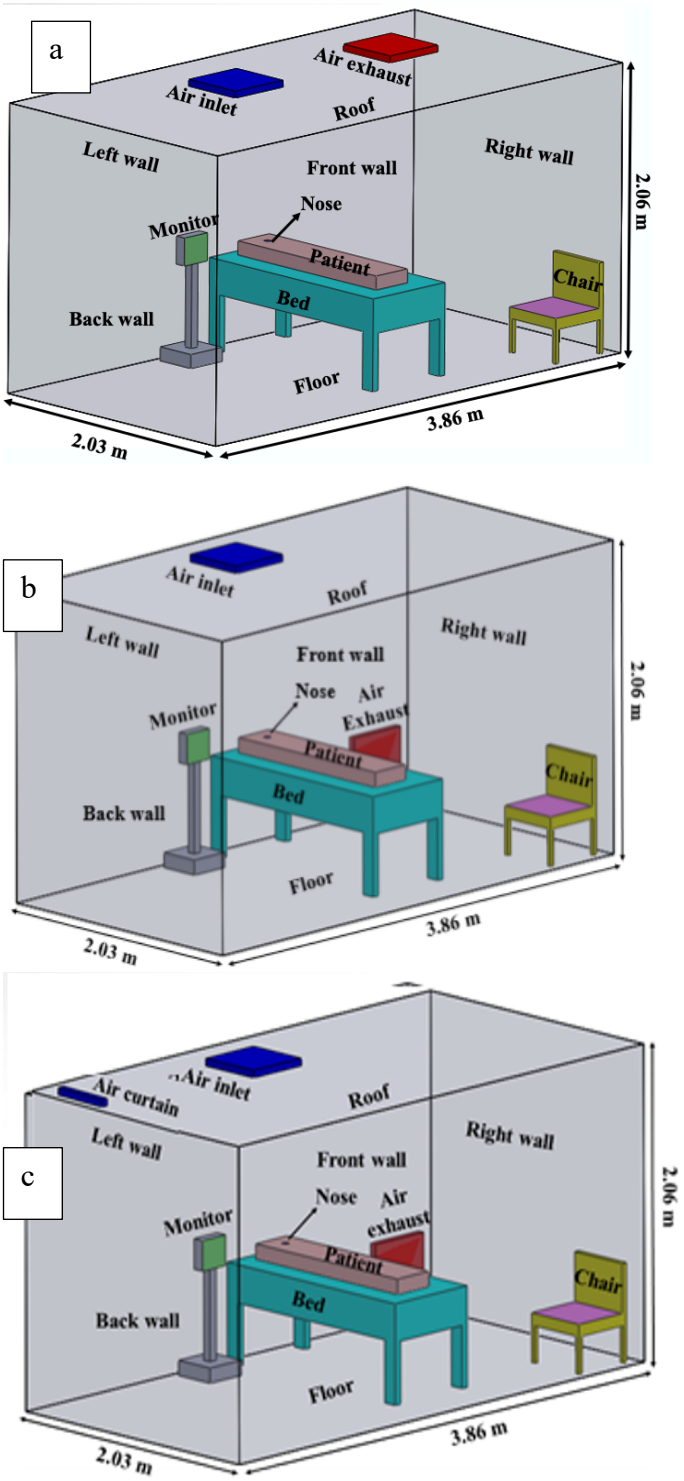

Figure 5 Hospital model room configurations a) with the air inlet in the ceiling on the left, exhaust on the right, showing the dimensions of the room and the positions of the objects in the room; b) Hospital model room configuration with the air inlet in

the ceiling above the bed, exhaust at the bottom left on the wall, showing the dimensions of the room and the positions of the objects in the room, and c) Hospital model room configuration with the air inlet in the ceiling above the bed, exhaust at the bottom left on the wall, air curtain entry/door showing the dimensions of the room and the positions of the objects in the room.

2.3.2. Sample assesment

For preliminary analysis of viable virus collection, each of the 12 filters collected in each test was placed in 2 mL of PBS. Aliquots of 4 mL of soft agar medium were added to glass tubes with 4 µL of 100 mg/mL Ampicillin. The tubes were submerged in 60 ^{o}C water to keep the medium for solidifying. 100 µL of a 10x dilution of each collected sample and 100 µL of the fresh mid-log phase *Salmonella typhimurium* LT2 RP1 host were added to the medium and poured over a plate. Of a 10^{-6} dilution of either the nebulized liquid or the stock solution 100 µL were added to the soft agar medium with 100 µL of the *Salmonella* host and poured over a TSA plate. The same was done with the exhaust filter. The plates were placed in the incubator overnight at 37 ^{o}C and the plaque forming units (PFUs) were counted the next morning. To assess the number of viable viral particles in the collected samples, cell tissue culture was used as described in section 2.2. Total BCoV numbers were quantitated by qPCR using BCoV specific primers and ABI qPCR chemistry as described in section 2.2.

2.3.3. Computational fluid dynamics (CFD) modeling and validation

HOBOware dataloggers were used for the continuous recording of temperature and relative humidity data at the bioaerosol collection sites. The airflow was measured within every cubic meter of the chamber by anemometry (TSI Inc., Burnsville, MN) to

validate the flow model [23,24]. The HOBOunits were connected to the 12 PM 2.5 samplers and started when the testing began. The data from the HOBOware was collected, exported and analyzed in Excel to get the total volume and air flow rate. SolidWorks was used to create a model of the hospital model room, bed, visitor chair, and monitor based on the dimensions provided by the mechanical blueprint of the chamber. A patient was modeled as a 51.75 in. long and 9.67 in. wide rectangular prism based off the average height and waist circumference of a male in the U.S [28]. This model was imported into ANSYS® Fluent software and used as the detailed mesh. Each model and mesh was adjusted based on the ventilation configuration being modeled. The mesh sized used for each simulation was 700,000 elementsThe standard k-ω turbulence model based on the Navier-Stokes equations was used to model unsteady room ventilation in steady flow conditions. Airflow through the space was simulated to determine virus movement in the room. For CFD simulation, in all ventilation configurations, the vertical walls, floor, monitor surface, hospital bed, chair, and air deflecting cones of the air diffuser were considered adiabatic. The transport equations, Eq. 1 and Eq. 2, used by ANSYS are shown below [29].

$$\frac{\partial}{\partial t}(\rho k) + \frac{\partial}{\partial x_i}(\rho k u_i) = \frac{\partial}{\partial x_j}\left(\Gamma_k \frac{\partial k}{\partial x_j}\right) + G_k - Y_k + S_k$$

Equation 1. Turbulence kinetic energy (k)

$$\frac{\partial}{\partial t}(\rho \omega) + \frac{\partial}{\partial x_i}(\rho \omega u_i) = \frac{\partial}{\partial x_j}\left(\Gamma_\omega \frac{\partial \omega}{\partial x_j}\right) + G_\omega - Y_\omega + S_\omega$$

Equation 2. Specific dissipation rate (ω)

The initial conditions used for the model are shown in Table 1 below. Velocity and temperature conditions were based on measurements taken during experimental testing. The air exchange rate for all models was 6 ACH and the door was closed in all configurations.

Table 1 Initial conditions used in ANSYS models.

Temperature	27 °C
Inlet	Velocity inlet (1.5 m/s)
Exhaust	Pressure outlet (0 atm)
Air curtain (config. 'c' only)	Velocity inlet (11.5 m/s)
Walls	No slip, stationary
Tolerance (x)	10^{-3}
Tolerance (y)	10^{-3}
Tolerance (velocity)	10^{-3}
Tolerance (k)	10^{-3}
Tolerance (ω)	10^{-3}
Tolerance (energy)	10^{-6}

2.4. Statistical Analysis

Statistical analysis was performed with Microsoft Excel (version 6.54) on all experimental data using ANOVA with a 95% confidence interval to determine if there was significant difference between replicates and experimental conditions for the plexiglass chamber and between replicates and ventilation configurations for the hospital model room.

3. RESULTS AND DISSCUSION

3.1. Plexiglass Model Chamber

Tests were conducted at 80% and 60% relative humidity at room temperature. Fig. 6 shows the total gene copy numbers (GCN) of BCoV per mL in the 80% relative humidity testing of the stock and nebulized solution samples quantitated by real-time qPCR testing. Figs. 7 and 8 show the total BCoV gene copy numbers (GCN) per L of Air of the aerosol samples collected by the wetted wall cyclone collectors and the MD8 Sartorius sampler and total BCoV gene copy numbers per cm^2 for the chamber and surface swab samples in the 80% relative humidity testing. Based on the results from the ANOVA test, all samples measured had significate difference between replicates with each p-value being below 0.05. Fig. 9 shows the total gene copy numbers (GCN) of BCoV per mL in the 60% relative humidity testing of the stock and nebulized solution samples quantitated by real-time qPCR testing. Figs. 10 and 11 show the total BCoV gene copy numbers (GCN) per L of Air of the aerosol samples collected by the wetted wall cyclones and the MD8 Sartorius sampler and total BCoV gene copy numbers per cm^2 for the chamber and surface swab samples in the 60% relative humidity testing. Based on statistical analysis performed, only the stock solution sample had significant difference between replicates with a p-value of 0.0448. Higher counts of BCoV were found in the 60% relative humidity testing samples compared to the 80% relative humidity testing samples. The WWC and MD8 Sartorius samples were the only sample sets found to have significantly different total BCoV gene copy numbers per sample collected. The p-value attained from the

ANOVA test between the 60% and 80% relative humidity tests for the WWC and MD8 samplers were 0.0147 and 9.30 x 10^{-5}.

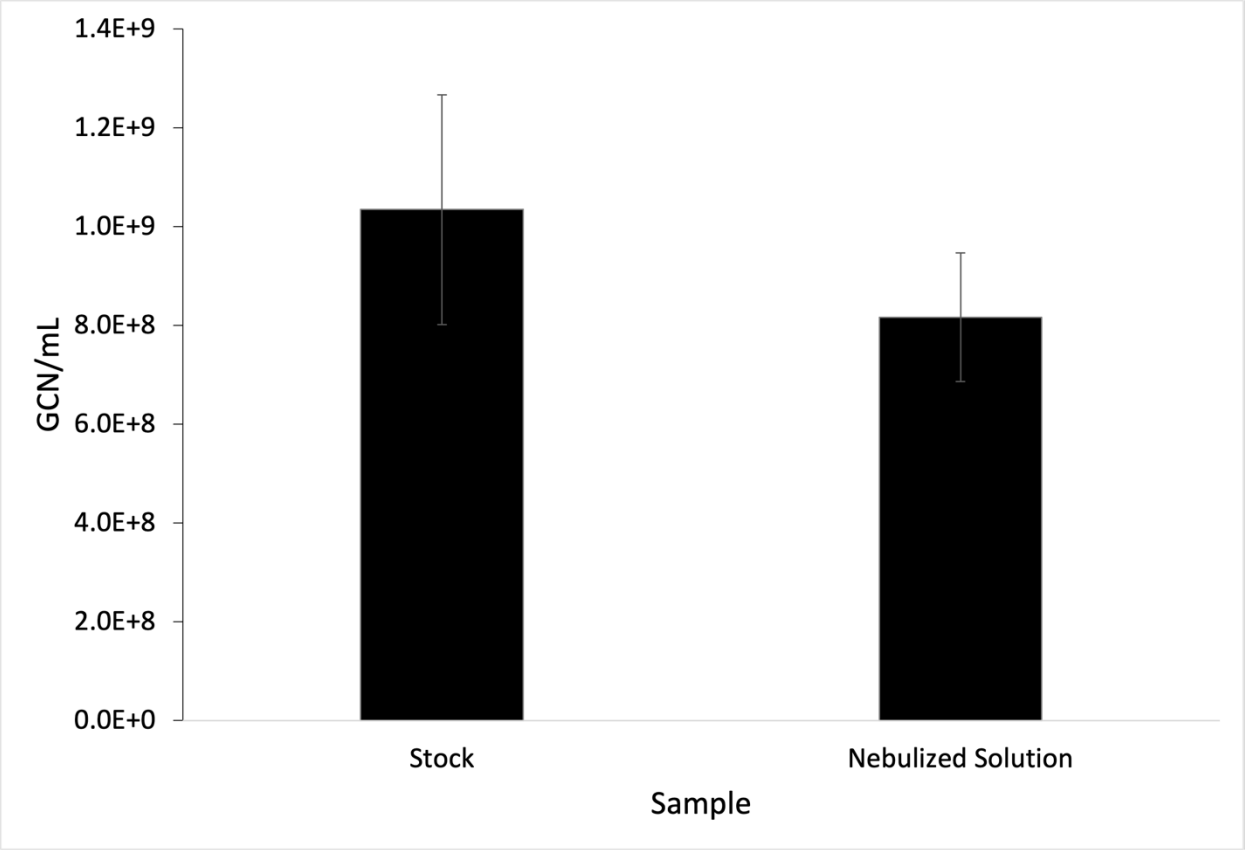

Figure 6 GCN/mL values of BCoV of the stock and nebulized solution samples at 25°C and 80% relative humidity.

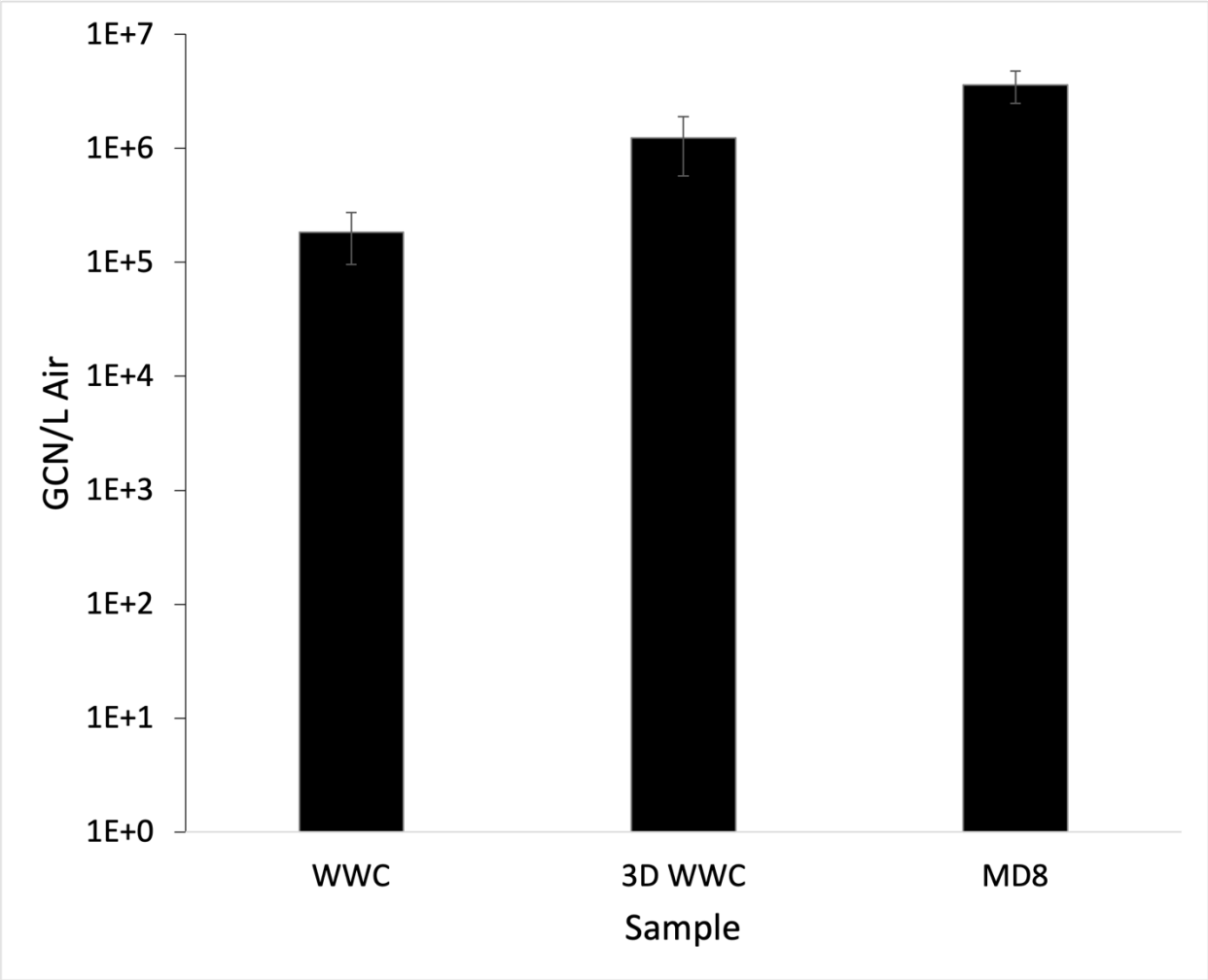

Figure 7 GCN/L Air of BCoV of aerosol samples collected by the Wetted Wall Cyclone (WWC), 3D Wetted Wall Cyclone (3D WWC), and the MD8 Sartorius (MD8) at 25℃and 80% relative humidity.

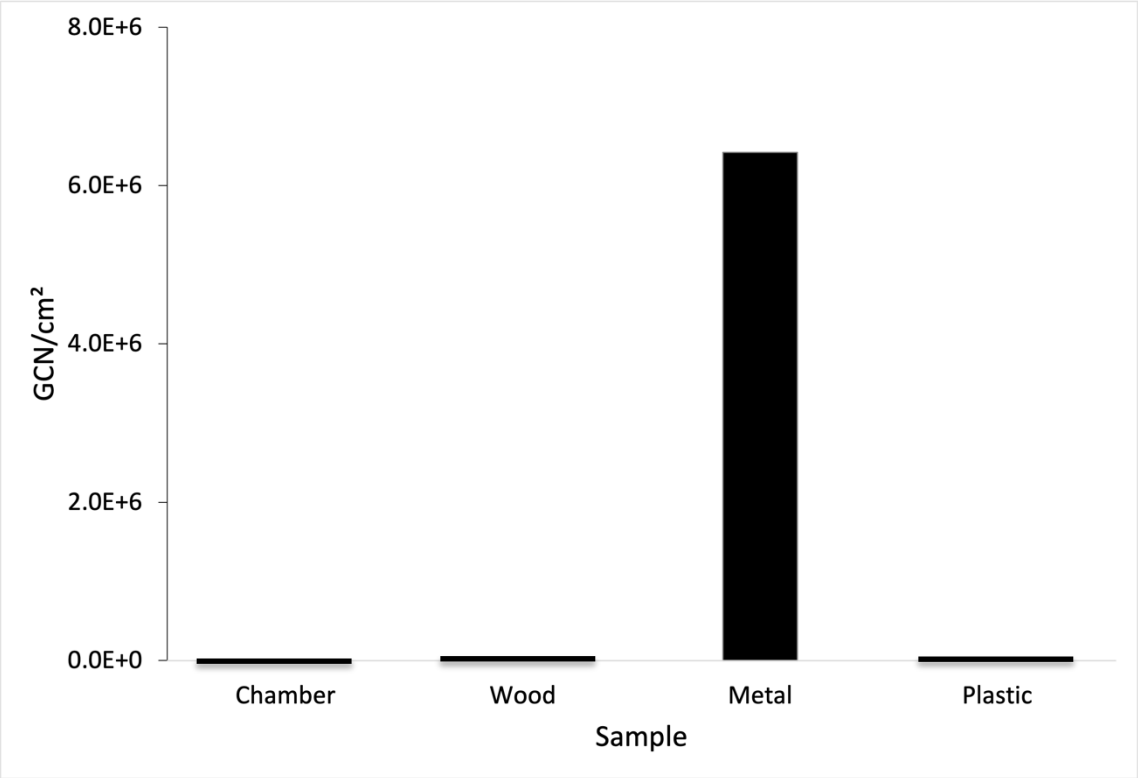

Figure 8 GCN/cm² of BCoV of the chamber swab, the wood, metal, and plastic surface swab samples at 25 ℃ and 80% relative humidity.

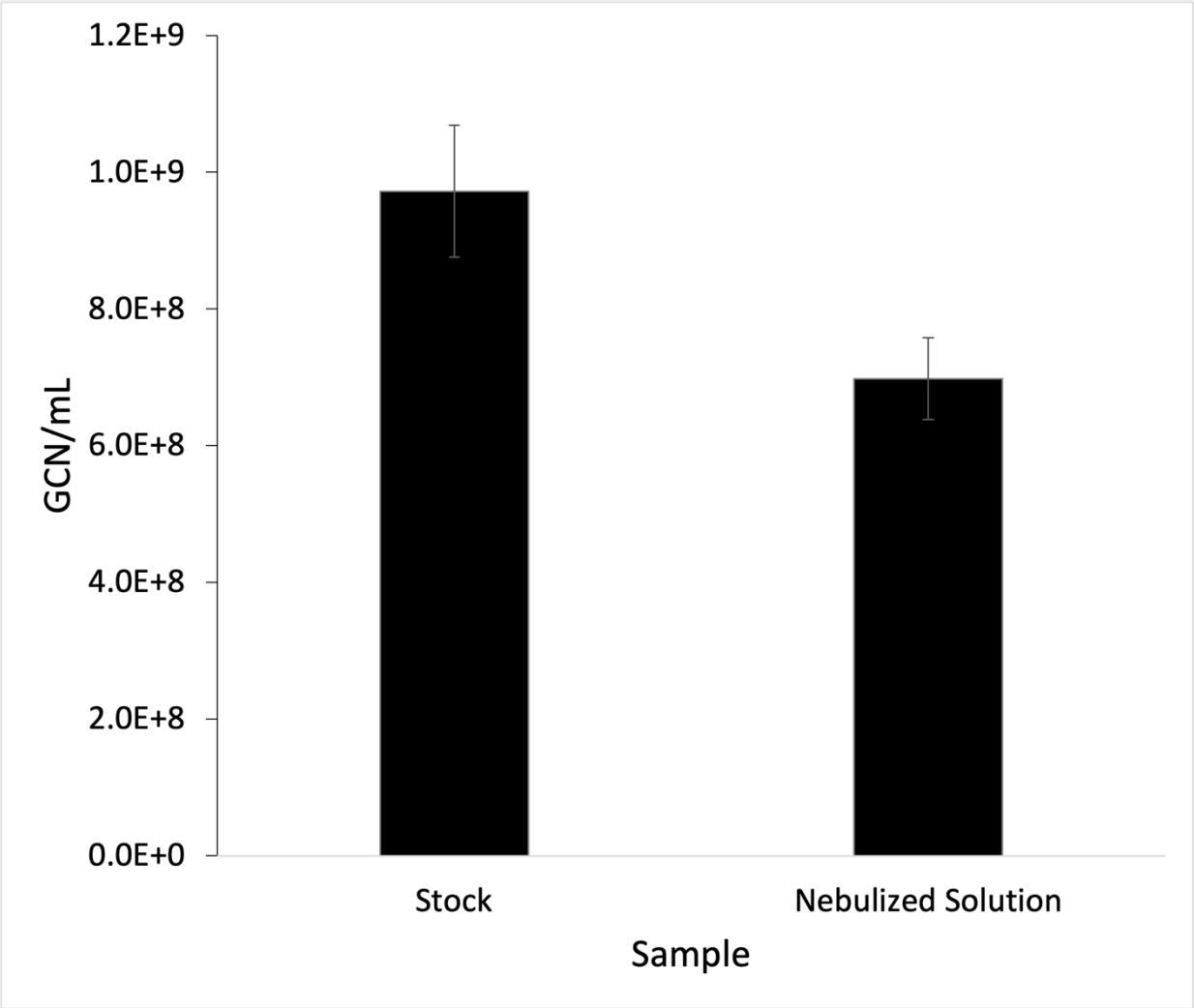

Figure 9 GCN/mL of BCoV of the stock and nebulized solution samples at 25℃ and 60% relative humidity.

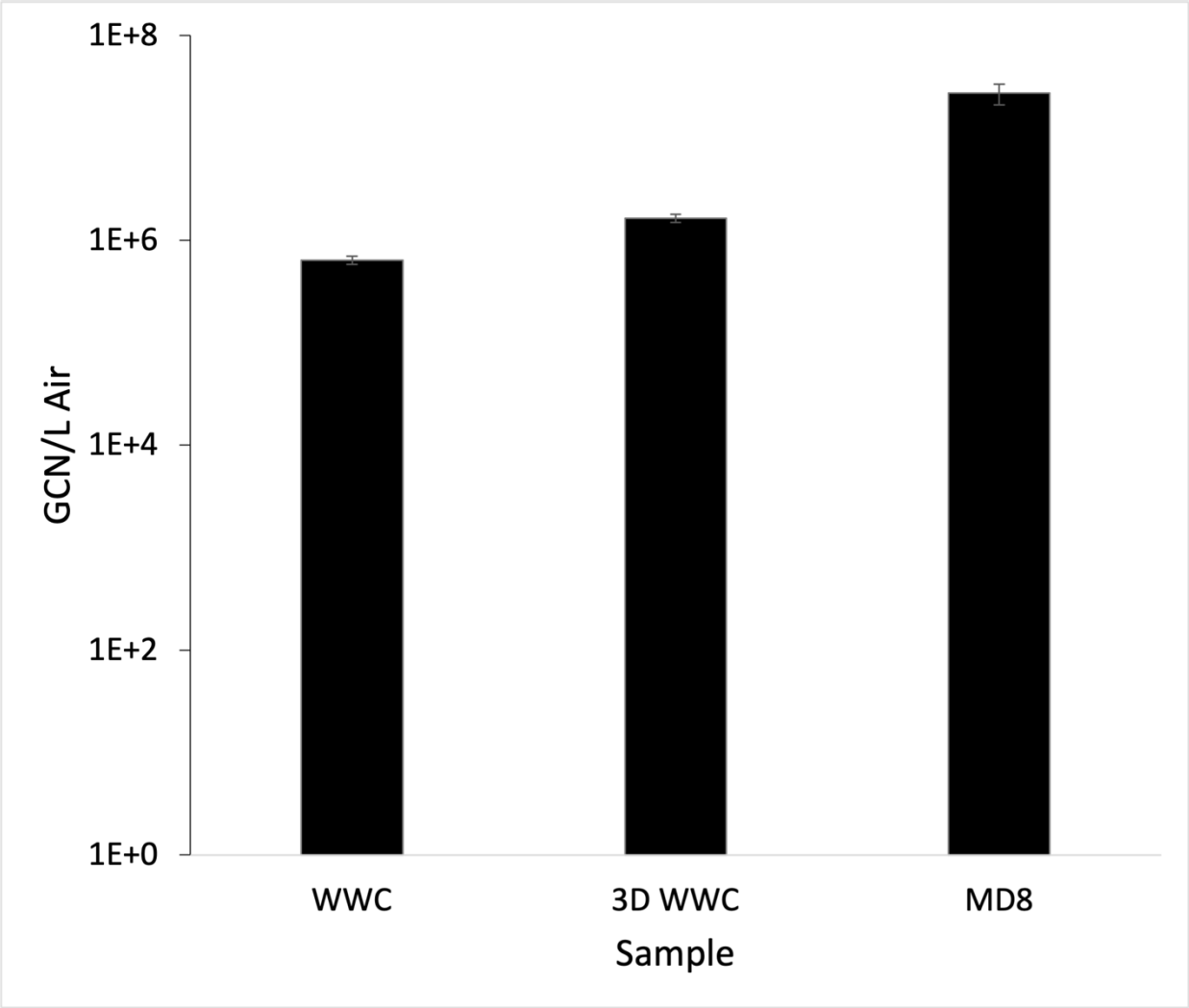

Figure 10 GCN/L Air of BCoV of aerosol samples collected by the Wetted Wall Cyclone (WWC), 3D Wetted Wall Cyclone (3D WWC), and the MD8 Sartorius (MD8) at 25°Cand 60% relative humidity.

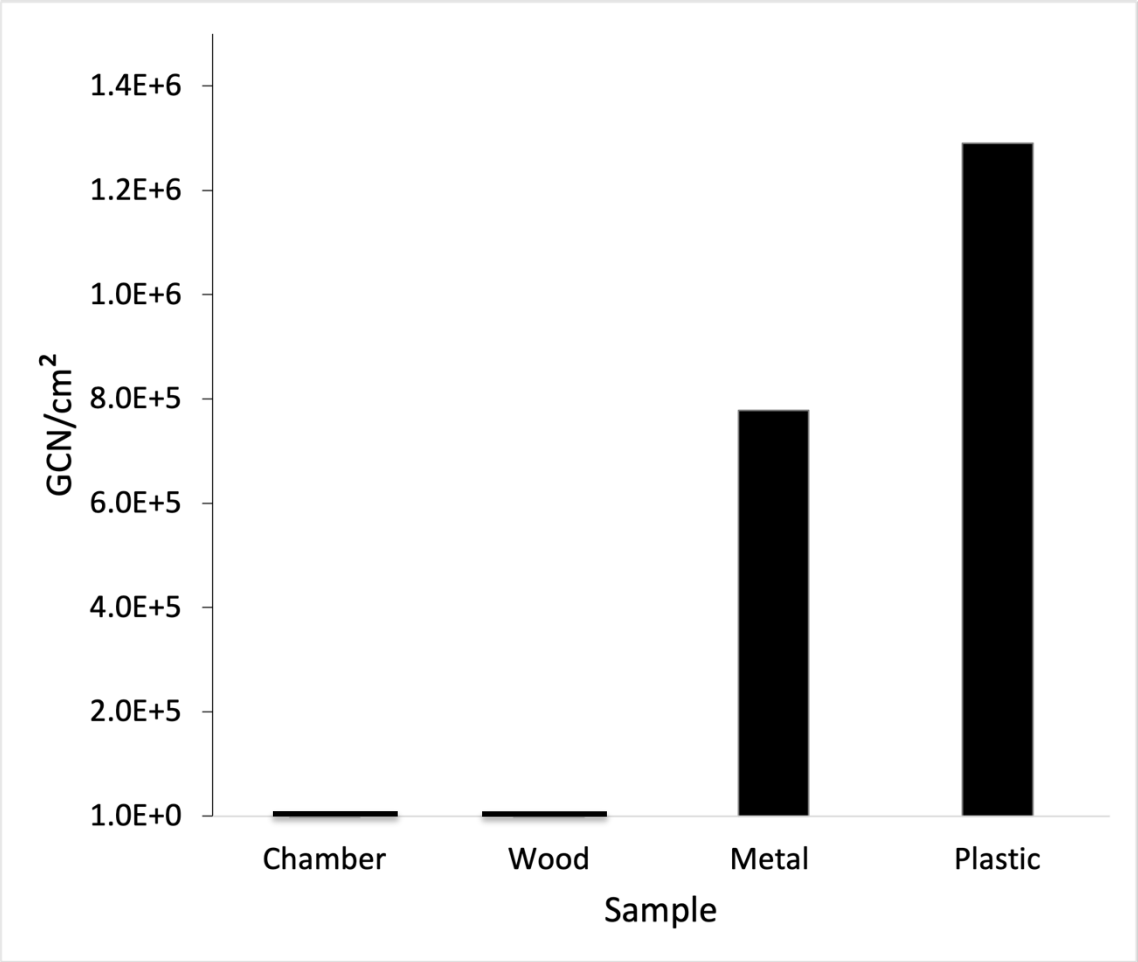

Figure 11 GCN/cm² of BCoV of the chamber swab, the wood, metal, and plastic surface swab samples at 25 °C and 60% relative humidity.

The results of BCoV association, Fig. 12, and dissociation, Fig. 13, to surfaces were obtained using the BLItz system. Fig. 12 shows the association constant for wood, metal, and plastic surface swab samples at 60% relative humidity, and 80% relative humidity. The ANOVA test performed comparing the different surface swab samples at 60% and 80% relative humidity returned p-values of 0.811 and 0.247. There was not significant difference between swab surface samples at 60% or 80% relative humidity.

Based on the ANOVA tests performed for each swab sample comparing the 60% and 80% results, there was no significant difference between the k_a at 60% and 60% relative humidity. Fig. 13 shows the dissociation constant for wood, metal, and plastic swab surfaces at 60% and 80% relative humidity. The ANOVA test performed comparing the different surface swab samples at 60% and 80% relative humidity returned p-values of 5.25×10^{-6} and 0.422. The was significant difference between the swab surface samples at 60% relative humidity but not at 80% relative humidity. The wood swab sample was the only surface sample with a significantly different k_d value between the 60% and 80% relative humidity tests. The p-value was 2.59×10^{-4}. The swab samples from metal and plastic exhibit stronger association at 80% relative humidity, though not enough difference to be significant. The swab sample from wood showed stronger dissociation at 80% relative humidity than at 60% relative humidity.

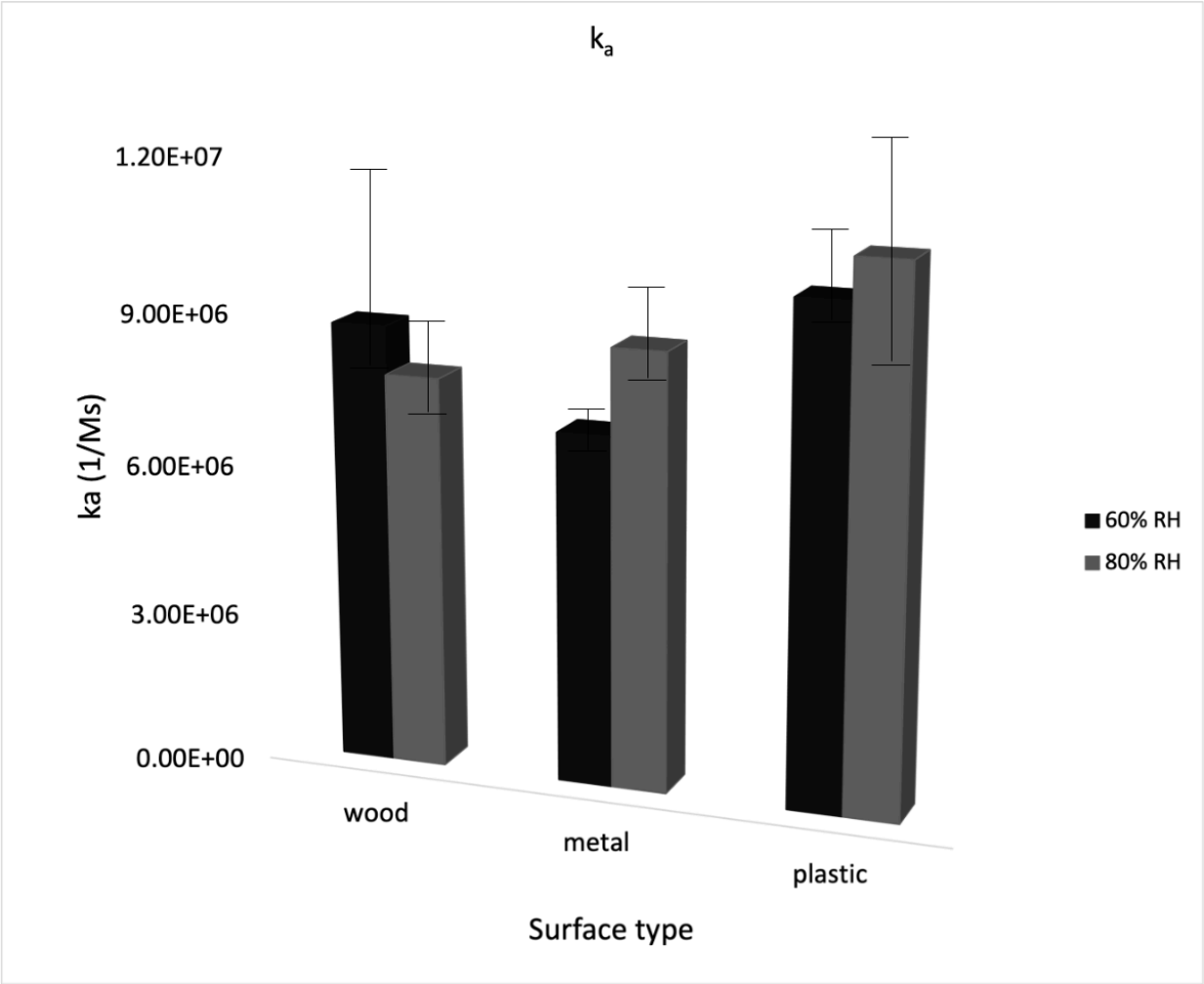

Figure 12 Association constants (k_a) of wood, metal, and plastic swab surface samples at 60% and 80% relative humidity, respectively.

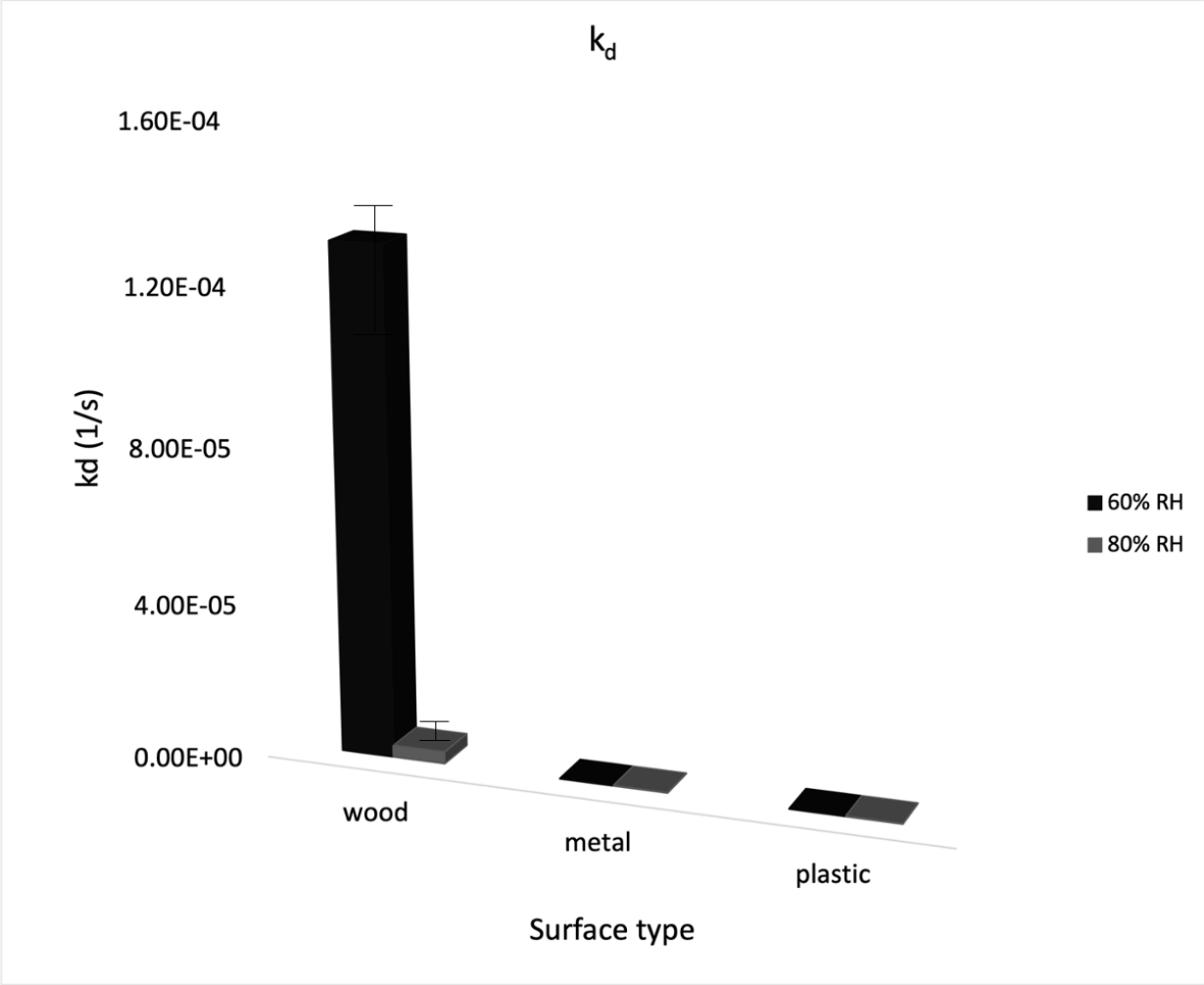

Figure 13 Dissociation constants (k_d) of wood, metal, and plastic swab surface samples at 60% and 80% relative humidity.

3.2. Hospital Model Room

Using configuration 'a' in Fig. 5, the particles were more concentrated around the door and the exhaust. The first test yielded a high number of virus aerosols collected at Sampler A, 1333 PFU/L air, which was significantly higher than the collections of the other samplers. The second test showed the highest concentration of particle collection at Sampler G, 620 PFU/L air. Both test 1 and test 2 resulted in high particle collection at the

door and on the bed, contrary to what was expected after the preliminary tests. Test 3 had high particle collection at the door, near the exhaust, and at the foot of the bed with the highest particle collection at Sampler K, 273 PFU/L air.

Fig. 14 shows the average particle flow based on the three tests. Due to the outliers in test 1 and test 2 there is higher average particle collection at Sampler A and Sampler G. The p-values obtained from ANOVA analysis suggested that there was no significant statistical difference between the 3 tests performed.

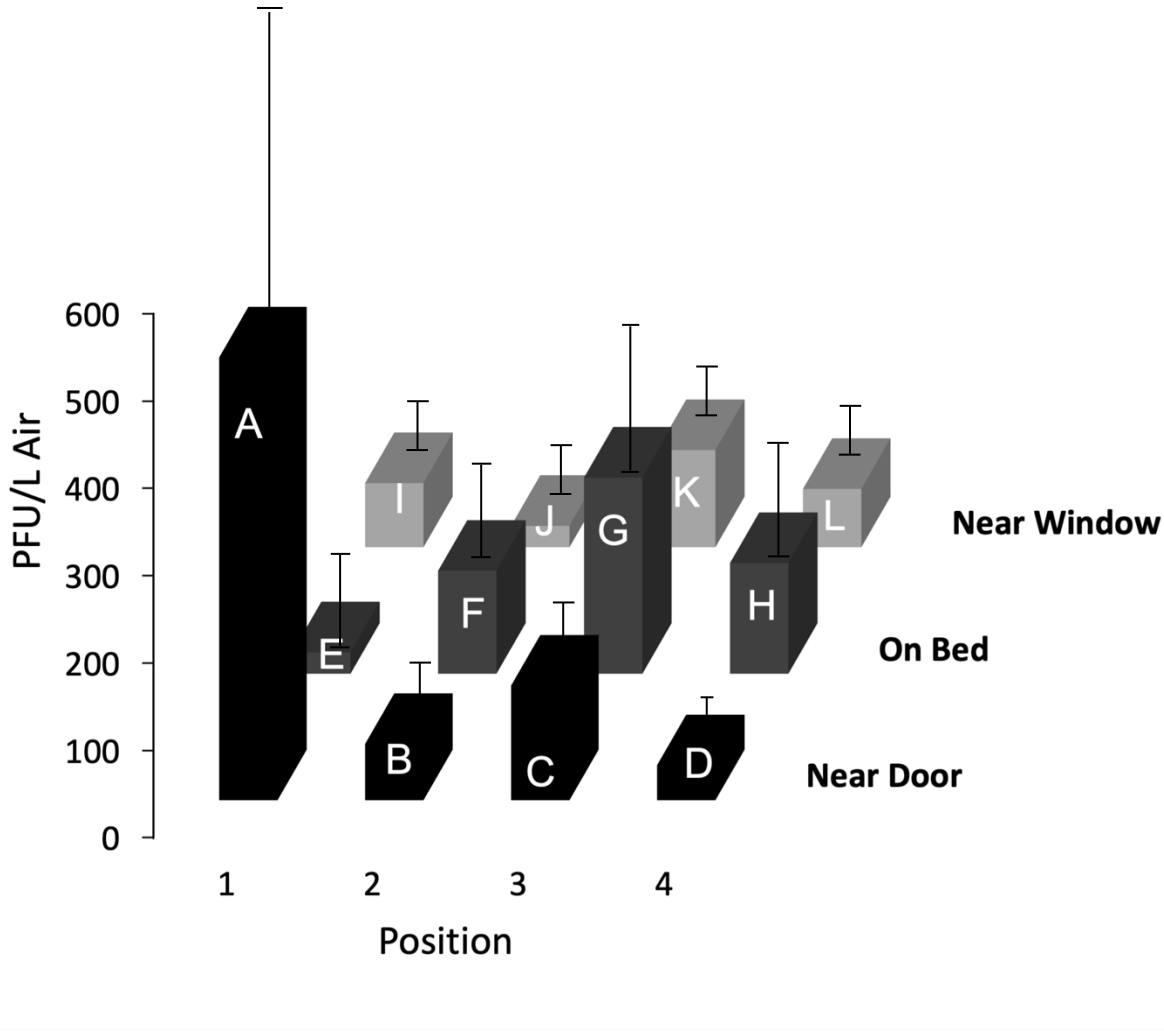

Figure 14 The average PFU/L air for each PM2.5 sampler at the location in the ¾ scale hospital model room using configuration 'a'.

Results from testing done using configuration 'b', without an air curtain, are shown in Fig. 15. The first test had the highest PFU/L Air at Sampler H, 8833 PFU/L Air, with the second highest at Sampler F, 4667 PFU/L Air. Sampler F consistently collected high numbers of PFU/L Air during all three tests. Fig. 15 shows the average particle flow based

on the three tests conducted using this configuration, with the highest average number of PFU/L Air collected at Samplers F and H, 3556 PFU/L Air and 3578 PFU/L Air. For this configuration, particles are more heavily concentrated at the patient's head, Sampler F, and feet, Sampler H. The p-values obtained from ANOVA analysis suggested that there was no significant statistical difference between the 3 tests performed.

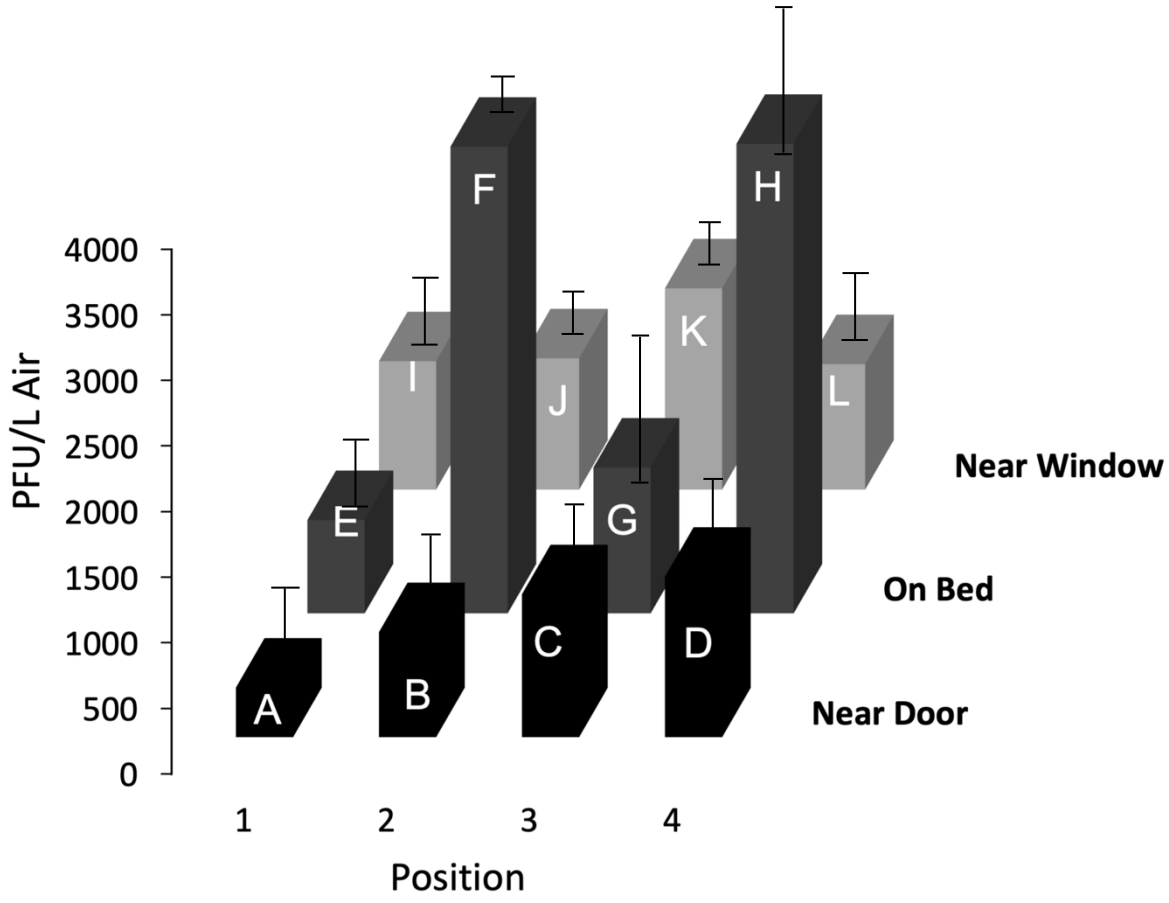

Figure 15 The average PFU/L air for each PM2.5 sampler at the location in the ¾ scale hospital model room using configuration 'b'.

The results from testing done using configuration 'c', with an air curtain, are shown in Fig. 16. The first test had highest PFU/L Air at Sampler F, 4347 PFU/L Air. Sampler F consistently collected high numbers of PFU/L Air during all three tests. Fig. 16 shows the average particle flow based on the three tests conducted using this

configuration, with the highest average number of PFU/L Air collected at Sampler F, 5600 PFU/L Air. For this configuration, particles were concentrated at the patient's head. The p-values obtained from ANOVA analysis suggested that there was no significant statistical difference between the 3 tests performed.

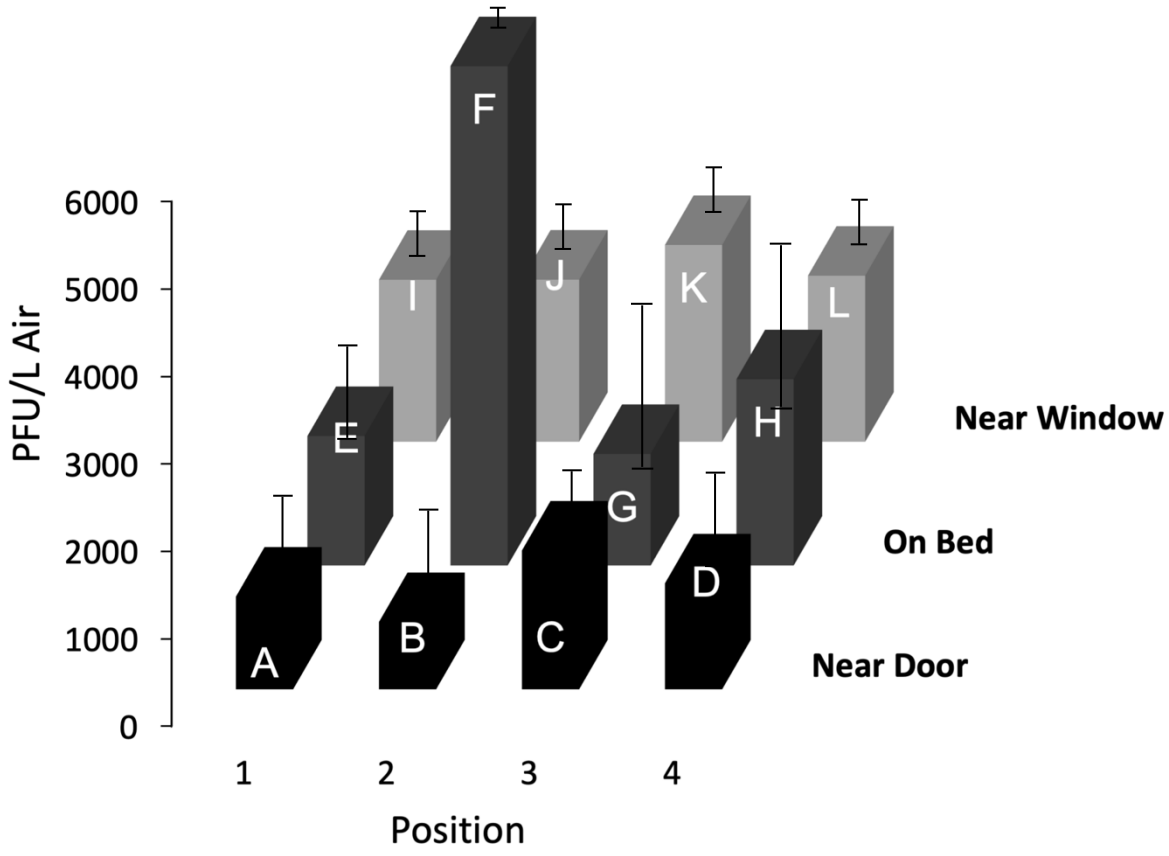

Figure 16 The average PFU/L air for each PM2.5 sampler at the location in the ¾ scale hospital model room using configuration 'c'.

Fig. 17 shows the average PFU/L Air graphs for all configurations normalized to the stock PFU counts of configuration ‘b’. Comparing the results, adding the air curtain decreases the concentration of particles at the patient’s head and throughout the room in comparison to without the air curtain in configuration ‘b’. Configuration ‘a’ decreased the particle concentration at the patient’s head but had the highest concentration at Sampler A by the door in the hospital test room. Based on the p-value, 0.832, obtained from the ANOVA test, there is not significant difference between the average results from the three configurations.

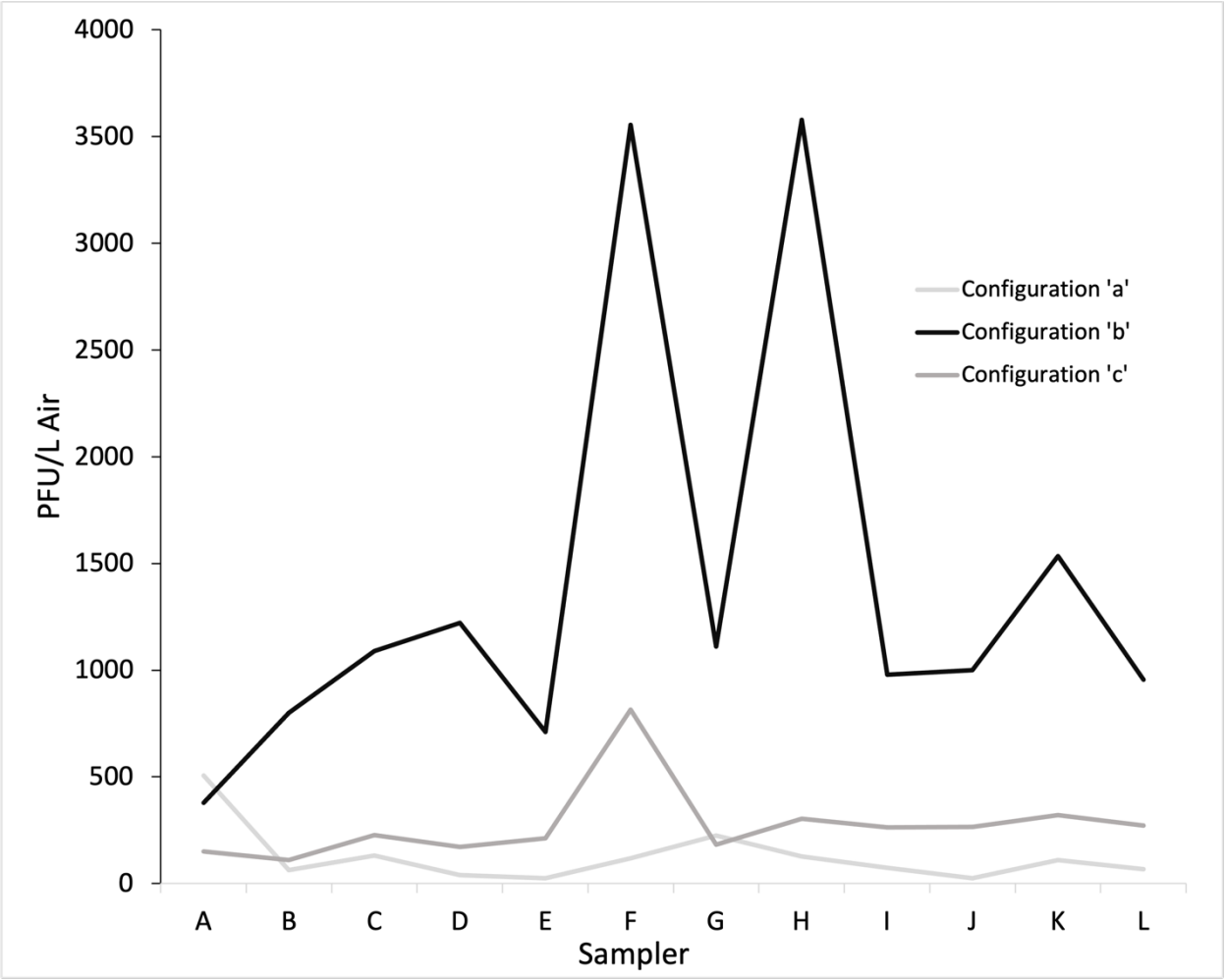

Figure 17 The average PFU/L Air at each sampler for each of the configurations, a, b, and c. All PFU/L Air counts were normalized based on the stock PFU counts from the configuration 'b' testing.

3.3. Air Modeling

The flow models in Figs. 18-20 show the air velocity streamlines under each of the configurations. Fig. 18, configuration 'a', shows many air vortices appearing at the door. The model for configuration 'b', Fig. 19, suggests the air remains at and moves around the door with few streamlines going toward the exhaust. The flow model shown in Fig. 20

demonstrates the air curtain pushing the air velocity streamlines away from the door with more streamlines exiting at the exhaust outlet.

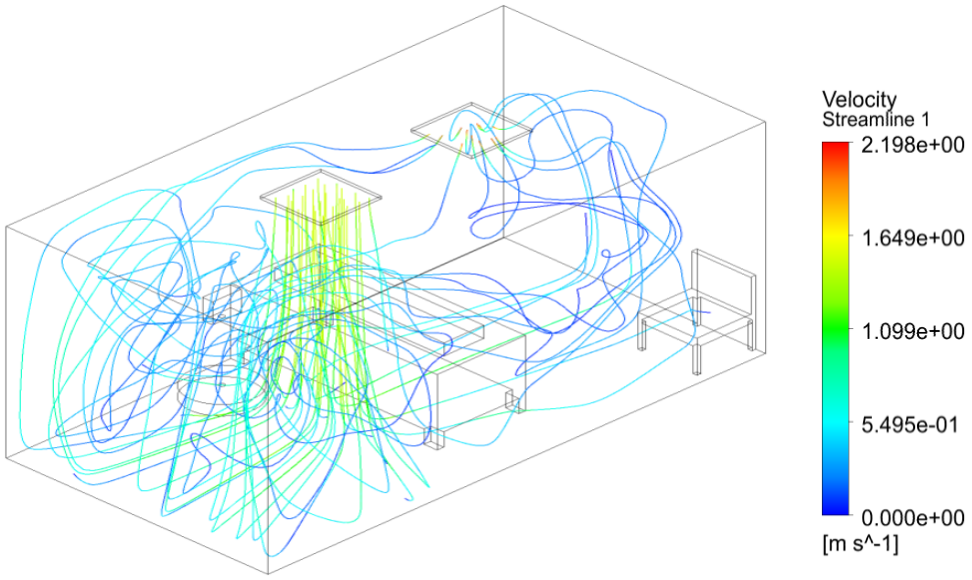

Figure 18 The computational flow model shows airflow velocity streamlines for configuration 'a'.

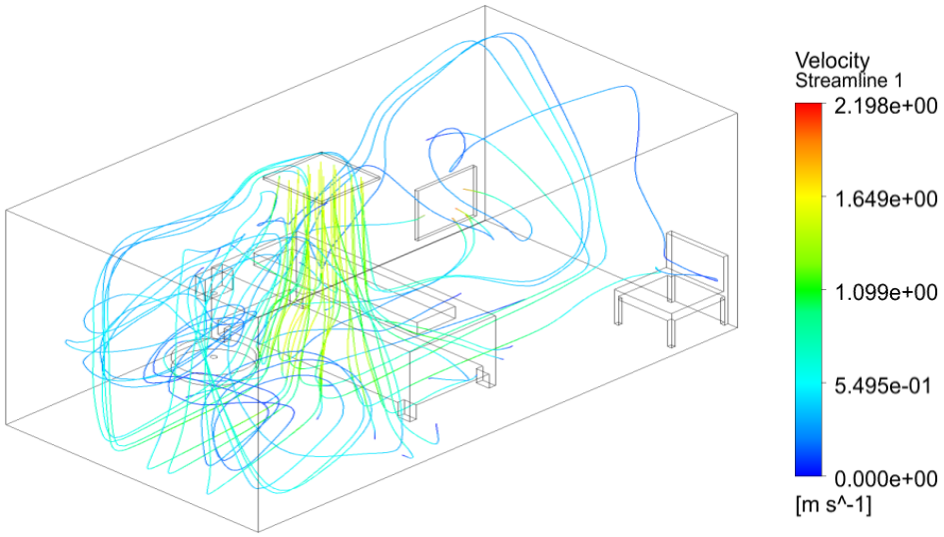

Figure 19 The computational flow model shows airflow velocity streamlines for configuration 'b'.

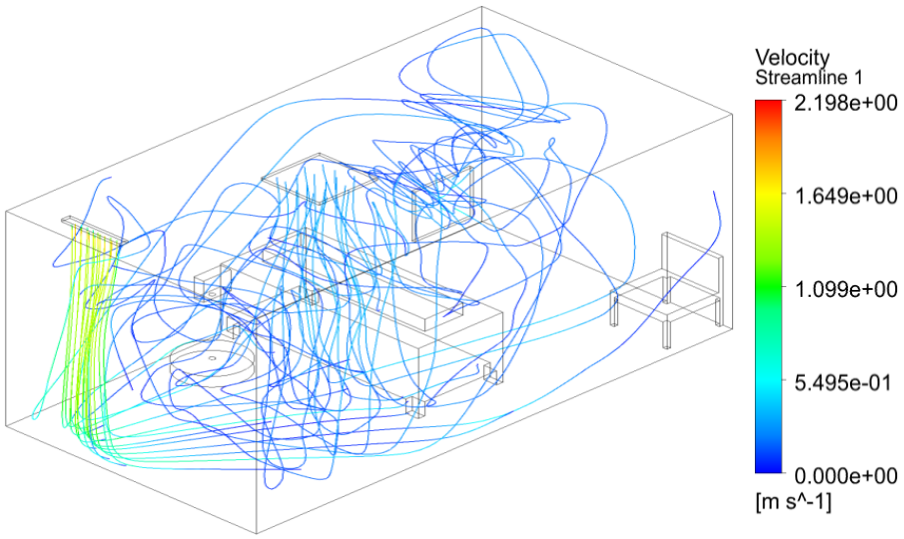

Figure 20 The computational flow model shows airflow velocity streamlines for configuration ‘c’.

4. CONCLUSIONS

Different air inlet and outlet combinations including installation of an air-curtain were tested to limit the spread of virus with the ventilation airflow. Effects of different ventilation geometries were shown on velocity patterns and the distribution of bioaerosols in the room. The results from the experimental data in the hospital test room correlate with the findings from the flow models. The addition of an air curtain leads to less turbulent air flow at the entrance and a decrease in virus particles remaining in a room. Highest phage concentration was detected at the patient's head, by sampler F, but concentration decreased significantly with the air curtain opposed to the configuration without it. Stronger virus association was found on plastic and metal surfaces and stronger dissociation was found from the wood surface at 80% relative humidity. Total counts of BCoV were higher at 60% relative humidity compared to 80% relative humidity. The results help recommend necessary changes in design to decrease residence time of contaminated air and to protect health care workers and visitors.

Future work will focus on viral particle tracking and movement under different environmental conditions within the plexiglass chamber. Additional testing will need to be completed in the hospital test room for longer periods with different air velocities to determine optimal air exchange rates.

REFERENCES

[1] WHO Coronavirus disease (COVID-2019) situation reports. Geneva: World Health Organization, 2020. (https://www.who.int/emergencies/diseases/novel-coronavirus-2019/situation-reports/).

[2] Chan, K. H., Peiris, J. S., Lam, S. Y., Poon L. L., Yuen, K. Y. and W.H. Seto. 2011. The Effects of Temperature and Relative Humidity on the Viability of the SARS Coronavirus. Adv Virol. 2011: 734690. doi: 10.1155/2011/734690

[3] Gerba, C. P. and W. Q Betancourt. 2017. Viral Aggregation: Impact on Virus Behavior in the Environment. Environ. Sci. Technol. 51: 13, 7318-7325. doi: 10.1021/acs.est.6b05835

[4] Ong, S. W. X., Tan, Y. K., Chia, P. Y., Lee T. H., Ng, O.T., Wong, M. S. Y. and K. Marimuthu. 2020. Air, surface environmental, and personal protective equipment contamination by severe acute respiratory syndrome coronavirus 2 (SARS-CoV-2) from a symptomatic patient. JAMA, doi:10.1001/jama.2020.3227

[5] van Doremalen, N., Bushmaker, T., Morris, D. H., Holbrook, M. G., Gamble, A., Williamson, B. N., Tamin, A., Harcourt, J. L., Thornburg, N. J., Gerber, S. I., Lloyd-Smith, J. O., de Wit, E. and V. Munster. 2020. Aerosol and Surface Stability of SARS-CoV-2 as Compared with SARS-CoV-1. New England Journal of Medicine. doi: 10.1056/NEJMc2004973

[6] Santarpia, J. L., Rivera, D. N., Herrera, V., Morwitzer, M. J., Creager, H., Santarpia, G. W., Crown, K. K., Brett-Major, D., Schnaubelt, E., Broadhurst, M. J., Lawler, J. V., Reid, St. P. and J. J. Lowe. 2020. Transmission Potential of SARS-CoV-2 in Viral Shedding Observed at the University of Nebraska Medical Center. Medrxiv. doi: 10.1101/2020.03.23.20039446v2

[7] Bourouiba, L. 2020. Turbulent Gas Clouds and Respiratory Pathogen Emissions: Potential Implications for Reducing Transmission of COVID-19. *JAMA.* Published online March 26, 2020. doi:10.1001/jama.2020.4756

[8] Han, Z. Y., Weng, W. G. and Q. Y. Huang. 2013. Characterizations of particle size distribution of the droplets exhaled by sneeze. Journal of the Royal Society, Interface, 10(88): 20130560. https://doi.org/10.1098/rsif.2013.0560

[9] Fabian, P., McDevitt, J. J., DeHaan, W. H., Fung, R. O. P., Cowling, B. J., Chan, K. H., Leung, G. M. and D. K. Milton. 2008. Influenza virus in human exhaled breath: an observational study. PLoS ONE, 3: e2691 (10.1371/journal.pone.0002691) [PMC free article] [PubMed] [CrossRef] [Google Scholar]

[10] Fabian, P., Brain, J., Houseman, E. A., Gern, J. and D. K. Milton. 2011. Origin of exhaled breath particles from healthy and human rhinovirus-infected subjects. J. Aerosol Med. Pulm. Drug Deliv. 24: 137–147. (10.1089/jamp.2010.0815) [PMC free article] [PubMed] [CrossRef] [Google Scholar]

[11] Vuorinen, V., Hellsten, A., Karvinen, A., Sironen, T. and P. Raback. 2020. https://www.aalto.fi/en/news/researchers-modelling-the-spread-of-the-coronavirus-emphasise-the-importance-of-avoiding-busy

[12] Han, Z., To, G. N., Fu, S. C., Chao, C. Y., Weng, W. and Q. Huang. 2014. Effect of human movement on airborne disease transmission in an airplane cabin: study using numerical modeling and quantitative risk analysis. BMC infectious diseases, 14: 434. doi: 10.1186/1471-2334-14-434

[13] Qian, H., and Zheng, X. 2018. Ventilation control for airborne transmission of human exhaled bio-aerosols in buildings. Journal of Thoracic Disease, 10(19), S2295–S2304. doi: 10.21037/jtd.2018.01.24

[14] Brown, L. 2020. Coronavirus found on Diamond Princess surfaces 17 days later. New York Post. Retrieved from https://nypost.com/.

[15] Setti, L., Passarini, F., de Gennaro, G., Barbieri, P., Pallavicini, A., Ruscio, M., Piscitelli, P., Colao, A. and A. Miani. 2020. Searching for SARS-COV-2 on Particulate Matter: A Possible Early Indicator of COVID-19 Epidemic Recurrence? *Accepted*, Int. J. Environ. Res. Public Health, 23 April 2020

[16] Bonilla, N., Rojas, M. I., Cruz, G. N. F., Hung S.H., Rohwer, F., and Barr, J. J. 2016. Phage on tap-a quick and efficient protocol for the preparation of bacteriophage laboratory stocks. PeerJ. Doi: 10.7717/peerj.2261

[17] Morawska, L. J. G. R, Ristowski, Z. D., Hargreaves, M., Mengersen, K., Corbett, S., Chao, C. Y. H., Li, Y. and D. Katoshevski. 2009. Size distribution and sites of origin of droplets expelled from the human respiratory tract during expiratory activities. Aerosol Science. 40: 256–269. doi: 10.1016/j.jaerosci.2008.11.002.

[18] Bellini, W. J. https://www.who.int/csr/sars/CDCprimers.pdf

[19] Lauterbach, S. E., Wright, C. M., Zentkovich, M. M., Nelson, S. W., Lorbach, J., Bliss, N., Nolting, J., Pierson, R., King, M. D., Bowman, A. S. 2018. Detection of influenza A virus from agricultural fair environment: air and surfaces. Preventive Veterinary Medicine, 153: 24-29. doi: 10.1016/j.prevetmed.2018.02.019

[20] King, M. D. and A. R. McFarland. 2012. Bioaerosol Sampling with a Wetted Wall Cyclone: Cell Culturability and DNA Integrity of Escherichia coli Bacteria. Aerosol Science and Technology, 46(1): 82–93.

[21] Oma, V.S., Tråvén, M., Alenius, S., Myrmel, M. and M. Stokstad. 2016. Bovine coronavirus in naturally and experimentally exposed calves; viral shedding and the potential for transmission. Virol. J. 13: 100. doi: 10.1186/s12985-016-0555-x

[22] Formosa, J. P. 2020. 3D printing PP (polypropylene) - why and how?, Magigoo. https://magigoo.com/blog/3d-printing-polypropylene-why-and-how/

[23] Laad, M. S. 2020. Chapter 15-Polymers in Sports, Polymer Science and Innovative Applications: Materials, Techniques, and Future Developments. Elsevier: 485-523. https://doi.org/10.1016/B978-0-12-816808-0.00015-9

[24] PMMA & Science. 2021. https://www.pmma-online.eu/pmma-science/

[25] Yang, T. Y., Riskowski, G. L. and A. Ch-Z. Chang. 2018. Effects of air relative humidity and ventilation rate on particle concentrations within a reduced-scale room. Indoor and Built Environment, 28(3): 335-344. https://doi.org/10.1177/1420326X18773134

[26] Drewry, J. L., Choi, C.Y. and J. M. Powell. 2017. Design and calibration of chambers for the measurement of housed dairy cow gaseous emissions. Transactions of the ASABE, 60(4): 1291-1300.

[27] Drewry, J. L., Mondaca, M., Luck, B. D. and C. Y. Choi. 2018. A Computational Fluid Dynamics Model of Biological Heat and Gas Generation in a Dairy Holding Area. Transactions of the ASABE, 61(2): 449-460. doi: 10.13031/trans.12394

[28] Centers for Disease Control and Prevention. 2021. *FASTSTATS - body measurements*. Centers for Disease Control and Prevention. https://www.cdc.gov/nchs/fastats/body-measurements.htm

[29] Ansys Fluent 12.0 theory guide - 4.5.1 standard - model. (n.d.). https://www.afs.enea.it/project/neptunius/docs/fluent/html/th/node66.htm